J. Membrane Biol. 66, 145–157 (1982)

The Journal of
Membrane Biology

Structure and Permeability of Goblet Cell Tight Junctions in Rat Small Intestine

James L. Madara and Jerry S. Trier
Departments of Pathology and Medicine, Brigham and Women's Hospital and Harvard Medical School, Boston, Massachusetts

Summary. Two major cell types, goblet and absorptive cells, dominate the epithelial lining of small intestinal villi. We used freeze-fracture replicas of rat ileal mucosa to examine the possibility that tight junction structure, known to relate to transepithelial resistance, might vary with cell type. Tight junctions between absorptive cells were uniform in structure while those associated with villus goblet cells displayed structural variability. In 23% of villus goblet cell tight junctions the strand count was less than 4 and in 30% the depth was less than 200 nm. In contrast, only 4% of absorptive cell tight junctions had less than 4 strands and only 9% had depth measurements less than 200 nm. Other structural features commonly associated with villus goblet cell tight junctions but less commonly with absorptive cell tight junctions were: deficient strand cross-linking, free-ending abluminal strands, and highly fragmented strands. Both *in vivo* ileal segments and everted loops were exposed to ionic lanthanum. Dense lanthanum precipitates in tight junctions and paracellular spaces were restricted to a subpopulation of villus goblet cells and were not found between villus absorptive cells. After exposure of prefixed ileal loops to lanthanum for 1 hour, faint precipitates of lanthanum were found in 14% of tight junctions and paracellular spaces between absorptive cells compared to 42% of tight junctions and paracellular spaces adjacent to villus goblet cells. When tested in Ussing chambers, the methods used for lanthanum exposure did not lower transepithelial resistance. Everted loops exposed to ionic barium and examined by light microscopy showed dense barium precipitates in the junctional zone and region of the paracellular space of villus goblet cells but not in these regions between absorptive cells. However, the macromolecular tracers, microperoxidase, cytochrome *c* and horseradish peroxidase, were excluded from both villus goblet cell and absorptive cell paracellular spaces in *in vivo* segments. These findings suggest that a subpopulation of villus goblet cells may serve as focal sites of high ionic permeability and contribute to the relatively low resistance to ionic flow which characterizes the small intestinal epithelium.

Key words tight junction · intestine · goblet cell · epithelial permeability

Introduction

The epithelial lining of mammalian small intestine is constantly renewed as senescent cells are sloughed from the tips of the villi and undifferentiated crypt cells proliferate and migrate onto the villus where they mature [35]. Not surprisingly, during this process the epithelial cells undergo extensive biochemical, functional and morphological alterations [5, 7, 10, 25, 27, 28, 30, 35] which include changes in tight junction structure [18]. While tight junctions of villus absorptive cells are rather uniform in structure, those between undifferentiated crypt cells are more variable and, on the average, have fewer strands and are less deep than those between villus absorptive cells [18]. Since epithelial permeability may be influenced by the complexity of tight junction structure [4], these features suggest that the crypt and villus epithelia may differ in transepithelial resistance to ionic flow [10, 18].

Although absorptive cells are the most abundant cell population of the villus epithelium, many mucus-secreting goblet cells are interposed between them [35]. Recently we presented preliminary data that tight junctions associated with villus goblet cells may, like those of undifferentiated crypt cells, be less uniform in structure than tight junctions associated exclusively with absorptive cells [18]. However, identification of goblet cell-associated junctions in replicas is not simple since 1) fortuitous fracture faces which facilitate goblet cell recognition by including both the tight junction and cross-fractured cytoplasmic mucus granules are infrequent and 2) fracture planes which split the lateral membranes of absorptive cells adjacent to a goblet cell may not reveal structural components of the goblet cell itself yet still represent a goblet cell-associated tight junction. Therefore, in our earlier study we did not quantitate differences in replicas of fractured tight junctions involving villus goblet cells as opposed to those involving only absorptive cells.

In this report we describe criteria which permit reliable identification of tight junctions associated with villus goblet cells in freeze-fracture replicas of rat ileum. We have applied these criteria to quantitate the structural features of villus goblet cell-associated

0022-2631/82/0066-0145 $02.60

tight junctions (which will be referred to as villus goblet cell tight junctions) and contrast them to tight junctions which involve only villus absorptive cells (which will be referred to as absorptive cell tight junctions). In addition, we used both ionic and macromolecular tracers to probe the possible functional significance of demonstrated variations in villus goblet cell and absorptive cell tight junction structure.

Materials and Methods

For all experiments, segments of distal ileum were excised from 200–250 g male Sprague-Dawley rats anesthetized with either ether or Nembutal®. All animals were fasted overnight prior to use.

Morphologic Techniques

Ileal mucosa from 5 animals was prepared for freeze-fracture and electron microscopy of thin sections. Tissues were fixed initially for 1 h for freeze-fracture and 2 hr for conventional electron microscopy at 4 °C in a solution of 2% formaldehyde, 2.5% glutaraldehyde and 0.4% $CaCl_2$ in 0.1 M Na cacodylate buffer [15]. Tissues for freeze-fracture were then embedded in 3% agar, and cut into 150 μm slices with a Smith-Farquhar tissue chopper. After equilibrating for 1 hr in a 20% glycerol in 0.1 M Na cacodylate buffer, tissue slices were mounted between two gold discs, rapidly frozen in partially solidified Freon®22, and stored in liquid nitrogen. Specimens were fractured at a stage temperature of −110 °C in a Balzers 300 freeze-etch device, replicated with platinum-carbon, cleaned in commercial bleach and mounted on formvar-coated 200 mesh hexagonal grids.

Villus goblet cell tight junctions and absorptive cell tight junctions were distinguished utilizing the criteria described in the Results section. For quantitative evaluation of tight junction structure, replicas of 20 randomly selected absorptive cell and 20 randomly selected villus goblet cell tight junctions were photographed at a magnification of 15,000×. Junctions at the extrusion zones of villus tips were avoided. These negatives were mounted on an illuminated viewing box and tight junction structure was analyzed using a 10× calibrated ocular micrometer. Average depth was determined by measuring the distance between the uppermost and lowermost strands one-fourth of the distance from each end of the exposed tight junction. Where wide expanses of tight junction were present a measurement in the center of the exposed junction was also taken. At the same points, *P* face strands and *E* face furrows intersecting the vertically placed micrometer bar were counted. A total of 53 sites were measured and counted for tight junctions from each cell type. Abluminal strands with unattached ends were counted separately for villus goblet and absorptive cell tight junctions and were expressed as the number of free-ending strands per linear μm of tight junction.

After initial aldehyde fixation tissues for conventional electron microscopy of thin sections were washed in 0.1 M Na cacodylate, postfixed for 1 hr in 1% osmium tetroxide, dehydrated in a graded series of alcohols, and embedded in epoxy resin. Oriented villi were selected from toluidine blue-stained 1-μm sections. Representative thin sections were mounted on copper mesh grids and stained with uranyl acetate and lead citrate.

Replicas and thin sections were examined and photographed in a Philips 300 electron microscope.

Tracer Experiments

Three buffers all at pH 7.4 when gassed with 95% O_2–5% CO_2 were used in these experiments. Buffer A contained (in mM): 114 NaCl, 5 KCl, 1.65 Na_2PO_4, 0.3 NaH_2PO_4, 25 $NaHCO_3$, 1.25 $CaSO_4$, 1.1 $MgSO_4$. Buffer B contained 124 NaCl, 5 KCl, 2.5 Hepes acid, 1.24 $CaCl_2$, 1.1 $MgCl_2$. Buffer C was identical to Buffer B except that 5 mM Tris replaced 2.5 mM Hepes acid.

Lanthanum Experiments. Twelve everted sacs from eight animals were prepared from distal ileum in the following manner: 8-cm lengths of ileum were gently flushed with Buffer A, ligated at one end, and everted over a glass rod; Buffer A with 10 or 50 mM glucose was instilled into the serosal cavity after which the remaining end was ligated. Sacs were then suspended in 300 ml of continuously oxygenated (95% O_2–5% CO_2) Buffer B or C to which 1 mM $LaCl_3$ had been added. After 20 min sacs were removed from buffer, submerged in fixative and samples were processed for electron microscopy. In all studies in which penetration of tight junctions by La^{3+} was evaluated, villi which showed the heaviest and most diffuse brush border labeling by La^{3+} were selected.

To determine if exposure of the ileal mucosa to 1 mM $LaCl_3$ for 20 min altered transepithelial resistance, ileal segments were removed from four rats, opened and the external longitudinal muscle layer was stripped away. The remaining tissue was mounted in Ussing chambers with 10 ml mucosal and serosal circulating reservoirs driven by a gas lift column of 95% O_2–5% CO_2. Buffer A with 50 mM glucose was placed in the serosal reservoir and Buffer C with 50 mM mannitol in the mucosal reservoir. After a 20-min equilibration period the transmucosal resistance was measured. One mM $LaCl_3$ was then added to the mucosal solution and the resistance was measured serially for 20 min. Identical measurements utilizing ileal mucosa not exposed to $LaCl_3$ from the same animals served as controls and permitted comparison of spontaneous fluctuations in transmucosal resistance that occurred during exposure to La^{3+}.

Preliminary experiments showed that considerable cellular damage occurred following incubation of everted sacs for longer than 20 min or in La^{3+} concentrations higher than 1 mM. To increase the degree of La^{3+} labeling and the duration of La^{3+} exposure without inducing cellular damage, six everted sacs prefixed by immersion in formaldehyde-glutaraldehyde fixative for 40 min to 1 hr were then suspended in a fixative containing 5 mM $LaCl_3$ for an additional hour. Tissues were then processed for electron microscopy. Unstained sections of villi from these sacs were examined to quantitate the relative frequency of La^{3+} penetration of tight junctions of absorptive cells and villus goblet cells. Tight junctions along the villus were scanned at a screen magnification of 20,000 using 10× oculars. Villus goblet cell tight junctions and villus absorptive cell tight junctions were scored as positive if they contained La^{3+} within the junction and/or the subjunctional intercellular space and negative if they did not. Tight junctions of cells at the base of the villus were not counted if La^{3+} failed to label the brush border at this level.

To determine whether prefixation alters resistance, four stripped ileal mucosal sheets were placed in Ussing chambers as described above. After a 20-min equilibration period, fixative was substituted for both mucosal and serosal buffers and transmucosal resistance was measured serially for 60 additional minutes.

The ileal mucosa of six additonal rats was exposed to La^{3+} *in vivo*. Ten-cm segments of distal small intestine were exposed and the ends were marked by passing surgical thread through the mesentery, taking care not to injure the vasculature. In three animals 1 ml of Buffer C containing 1 mM $LaCl_3$ was injected into the lumen through a 29 gauge needle at the proximal end of each segment. Twenty minutes later the segment was rapidly removed, opened, immersed in fixative and samples were processed for electron microscopy. In addition, freeze-fracture replicas were prepared and examined from these tissues. The remaining three animals were treated in a similar manner; however, each received additional 1-ml injections of 1 mM $LaCl_3$ after 15 and 45 min and tissue samples were harvested 60 min after the first $LaCl_3$ injection.

Barium Experiments. Since processing for electron microscopy probably leaches ionic tracers from the tissues and may create diffusion artifacts, we also exposed tissue to Ba^{2+} which, after brief fixation, can be precipitated as a rhodinozate salt and observed immediately by light microscopy [6, 38]. Everted sacs containing Buffer A and 10 mM glucose in the serosal compartment were suspended in an oxygenated solution composed of 90 mM $BaCl_2$, 5 mM $CaCl_2$ and 10 mM mannitol at pH 7.4 for 15 min. Sacs were fixed in 10% neutral phosphate-buffered formalin for 20–30 min chopped into 150-μm slices, immersed in saturated potassium rhodinozate solution, briefly rinsed in water, placed on glass slides, and examined for characteristic red-brown barium rhodinozate deposits by light microscopy.

Macromolecular Tracers. Ileal segments were marked *in vivo* with surgical thread in nine additional animals. Macromolecular tracers were dissolved in Buffer A and 1 ml was injected into the lumen at the proximal end of the segment, after 0, 15 and 45 min. Tissues were then removed and immersed in fixative 60 min after the first tracer injection. Groups of three animals were exposed to 0.5% microperoxidase (Sigma, molecular weight 1,900), 0.5% cytochrome *c* (Sigma Type VI, molecular weight 12,300), and 0.1% horseradish peroxidase (Sigma Type II, molecular weight, 40,000). Tissues were processed as previously described to demonstrate the tracers in thin sections (microperoxidase [9], cytochrome *c* [16], horseradish peroxidase [12]). Epithelial cell tight junctions and intercellular spaces were assessed for penetration by the tracer molecule by examination of unstained thin sections.

Results

Identification of Villus Goblet Cells and Their Associated Tight Junctions in Freeze-Fracture Replicas

In thin sections, goblet cells are readily identified by their characteristic large mucus granules (Fig. 2*C*); such granules occasionally identify goblet cells in freeze-fracture replicas (Fig. 1). More often, mucus granules are not revealed by cytoplasmic cross-fracture, hence other criteria must be used to identify goblet cells in replicas. Since they are shaped like a brandy goblet, the lateral membrane of villus goblet cells is convex while the lateral membrane of adjacent absorptive cells is concave (Fig. 1). In contrast, the lateral membranes of absorptive cells which abut one another are more or less flat. The microvilli of villus goblet cells vary in length and have few *P* face intramembrane particles (*IMPs*) whereas the microvilli of absorptive cells are approximately equal in length and have abundant *P* face *IMPs* (Fig. 2*A*) [18]. Caveolated cells are the only other villus epithelial cells which have few *P* face *IMPs* [18] but their wide microvilli and their characteristic microvillus tuft [26] permits them to be distinguished from villus goblet cells. Additionally, villus goblet cells frequently have a collar-like outpouching of apical cytoplasm which encircles the cell just below the tight junction in the region of the belt desmosome. This forms a bulge in the goblet cell lateral membrane and a complementary depression in the lateral membrane of adjacent absorptive cells (Fig. 2). On the villus, this collar-shaped

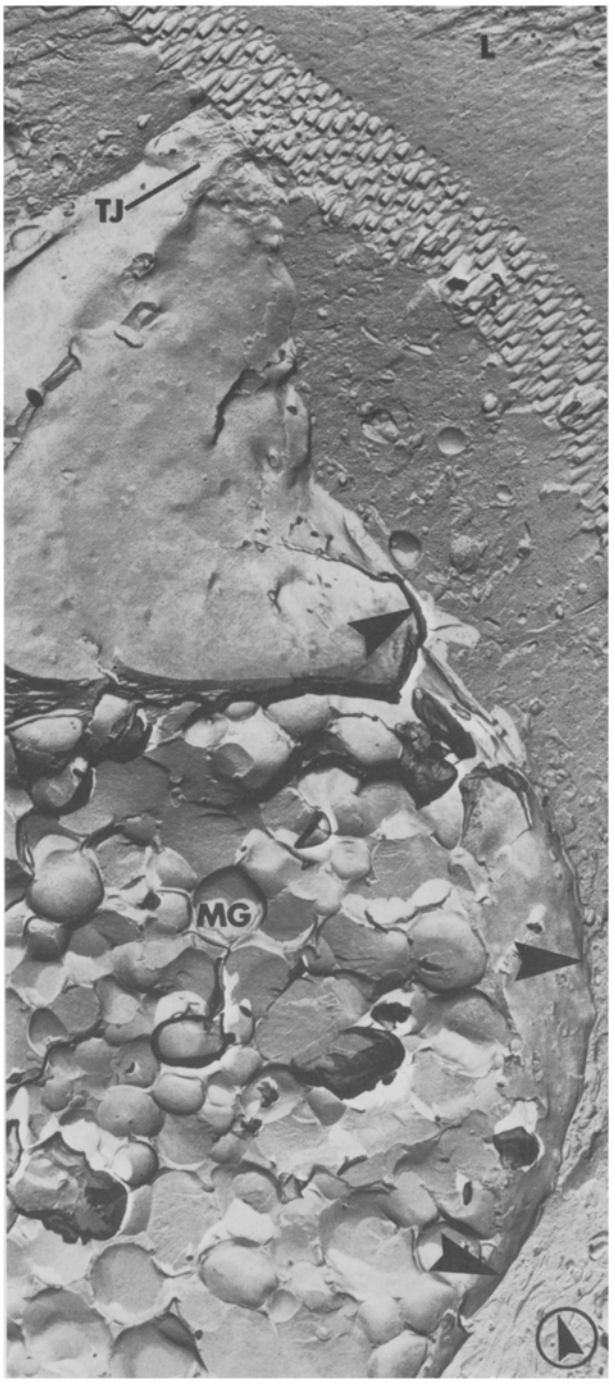

Fig. 1. Freeze-fracture replica showing lateral membrane of a villus goblet cell with typical brandy goblet bulge (arrowheads). Cytoplasmic cross fracture reveals many mucin granules (*MG*). The tight junction (*TJ*) lies adjacent to the lumen (*L*). The circled arrowhead in the lower right-hand corner of this and subsequent freeze-fracture replicas indicates the direction of platinum shadowing. (11,000×)

irregularity in the lateral membrane fracture face was observed only in goblet cells and on that portion of the lateral membrane of adjacent absorptive cells which was in direct contact with the goblet cell.

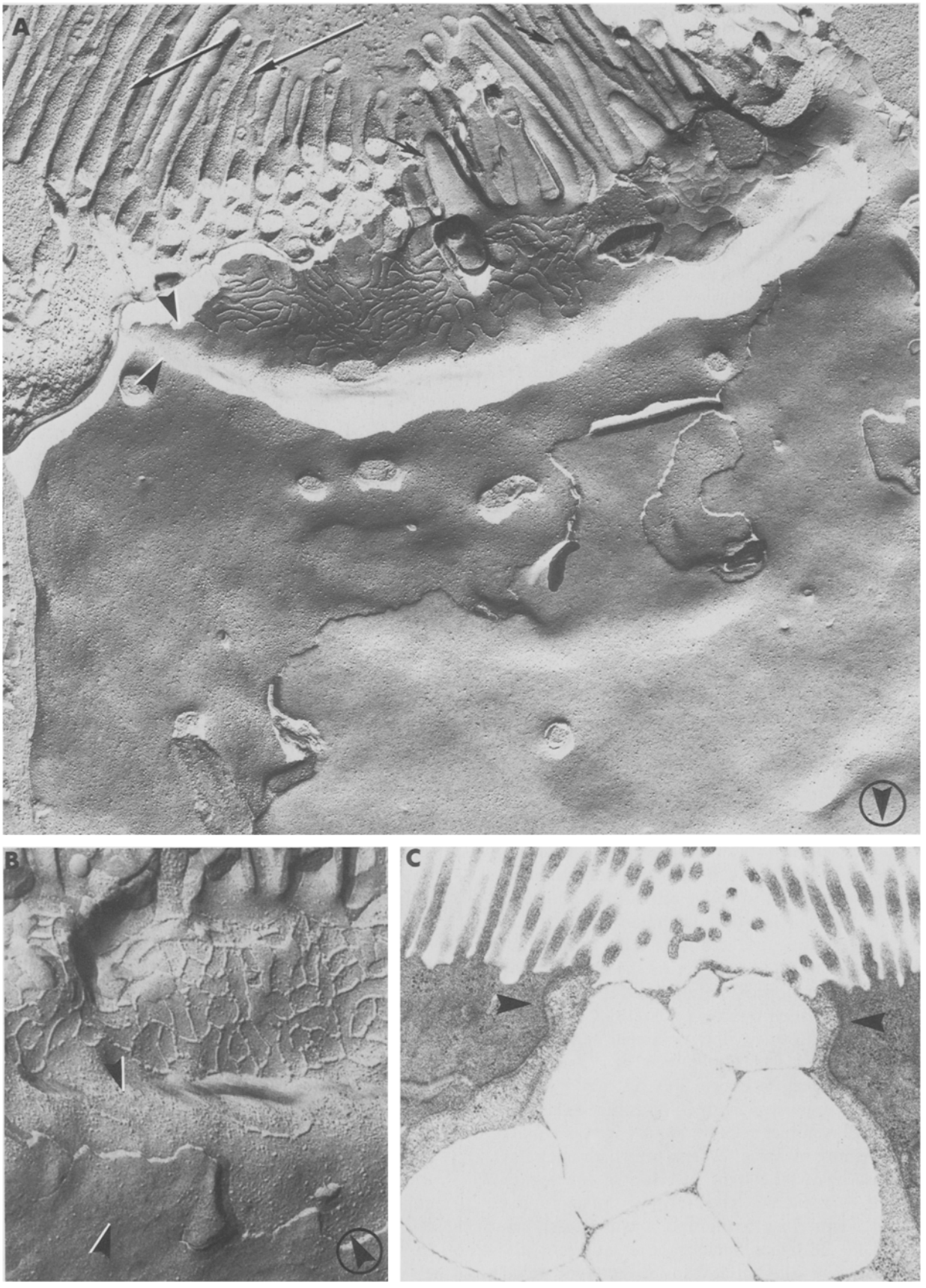
A
B
C

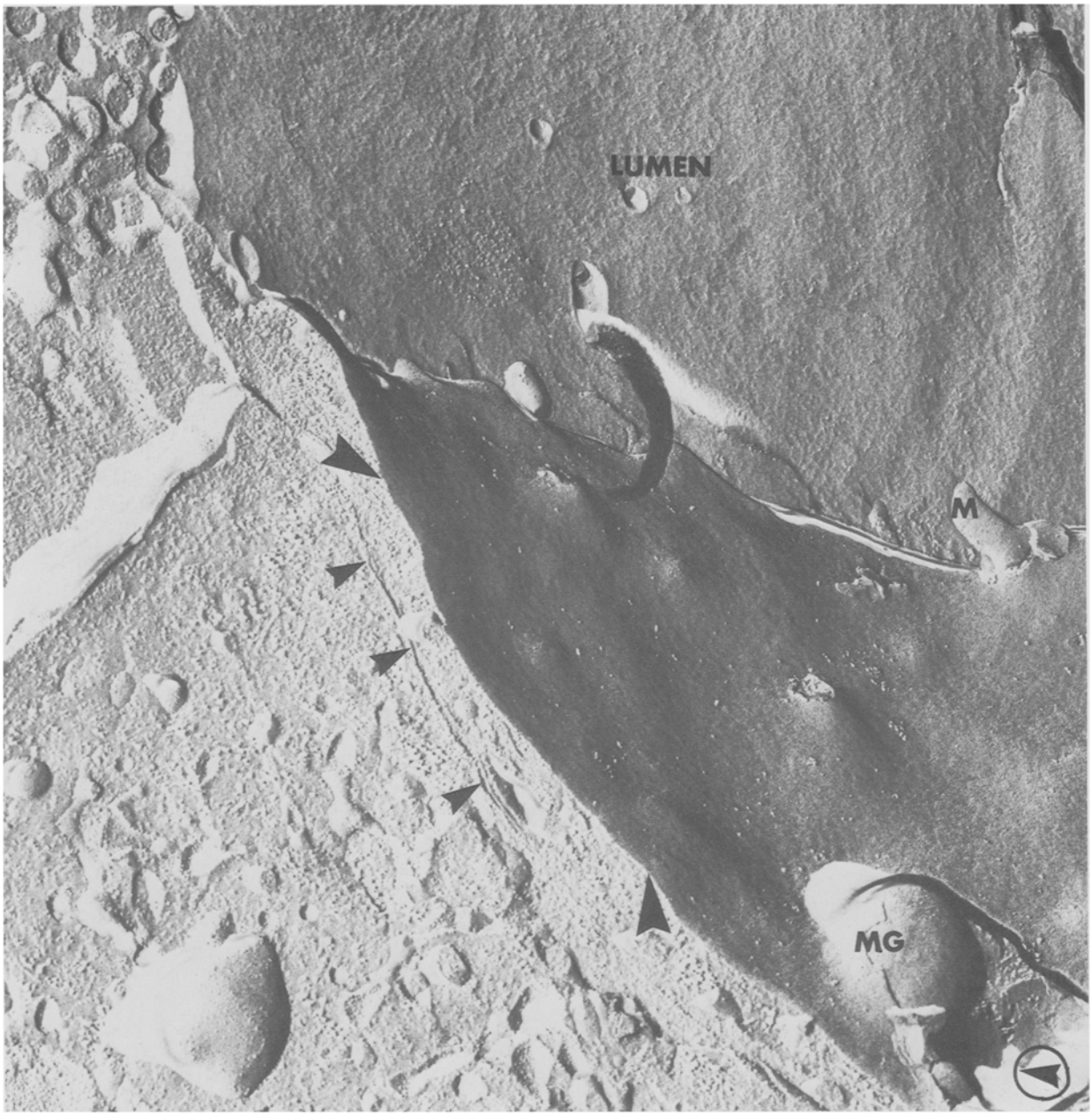

Fig. 3. Replica of villus goblet cell with cup-like indentation of apical membrane following secretion of apical cytoplasmic mucus granules. The fracture plane travels down the apical membrane (large arrowheads) and cross fractures into the membrane of an underlying cytoplasmic mucus granule (*MG*) Goblet cell microvilli (*M*) can be seen at the rim of the apical membrane cup. A thin rim of peripheral cytoplasm separates the apical membrane from the intercellular space (small arrowheads). To the left, the cytoplasm of an adjacent absorptive cell is revealed in cross-fracture. The misshapen apical membrane does not contain a tight junction, desmosomes or other junctional elements and should not be mistaken for a tight junction free lateral membrane. (50,000×)

Fig. 2. (facing page) (A) Replica of villus goblet cell showing a loosely woven net-like tight junction. Irregular microvilli with particle-poor *P* faces (short arrows) distinguish this cell from adjacent absorptive cells which have microvilli with particle-rich *P* faces (long arrows). In addition, the bulging lateral membrane and subjunctional collar-like outpouching of the lateral membrane (arrowheads) are characteristic of villus goblet cells. (41,000×). (B) Replica of villus goblet cell showing lateral membrane collar (arrowheads) immediately below the tight junction. (80,000×). (C) Electron micrograph of the apical aspect of a sectioned villus goblet cell showing outpouching of the lateral membrane (arrowheads) corresponding to the subjunctional lateral membrane collar seen in freeze-fracture replicas. (28,000×)

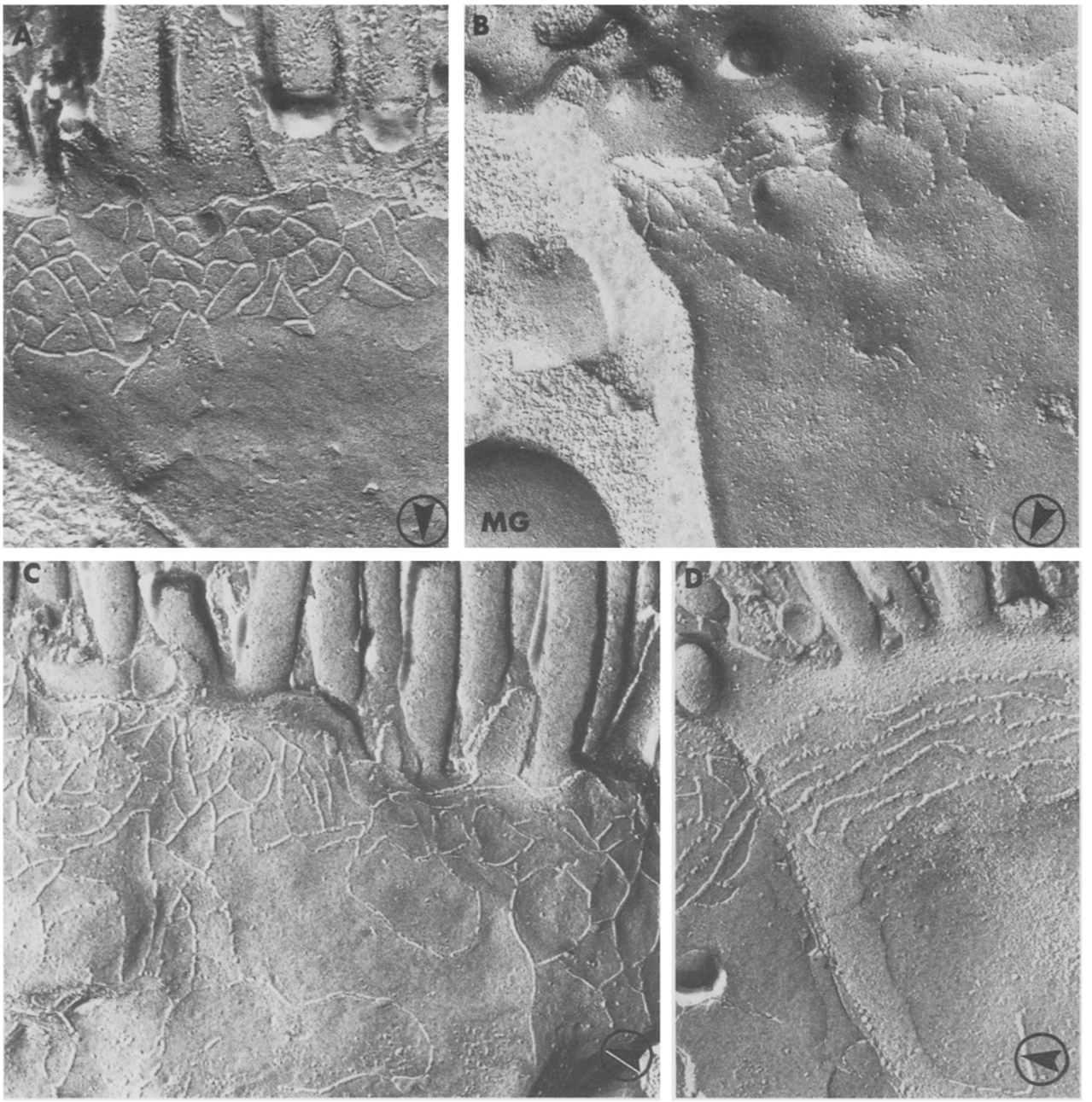

Fig. 4. (A) Replica of a tight junction between adjacent absorptive cells. The junction is uniform in depth and strand number and lacks meandering loose-ending abluminal strands. (B) Replica of villus goblet cell identified as such by the mucus granule (*MG*) seen at a zone of cytoplasmic cross-fracture. The tight junction is shallow and is composed of highly fragmented strands. Meandering loose-ending abluminal strands are frequent. (C) Replica of villus goblet cell identified as such by particle-poor microvillus *P* faces. The tight junction is quite deep and has strands which are very loosely interwoven. (D) Replica of villus goblet cell identified as such by particle-poor microvillus *P* faces. The tight junction is similar in depth and horizontal strand count to the absorptive cell tight junction shown in *A* but is fragmented and lacks crosslinking strands. (all 76,000 ×)

Some degree of caution is needed in identifying the lateral membrane of goblet cells. After release of the contents of superficial mucus granules, the goblet cell apical membrane becomes concave, forming a cup-like depression which extends into the apex of the cell [35]. If this membrane is followed along its fracture plane it could be misidentified as a lateral membrane free of any tight junction component (Fig. 3). It is distinguished from the lateral membrane by the absence of desmosomes and the low density

of *P* face *IMPs* (Fig. 3). Such misinterpretation may account for a previous description of small intestinal epithelial cells free of tight junction elements [33].

Goblet Cell Tight Junction Structure in Freeze-Fracture Replicas

The depth and strand numbers of tight junctions of absorptive cells are quite uniform (Fig. 4*A*). In contrast, those of villus goblet cells show substantial variation in depth and strand number (Fig. 4*B*, *C* and *D*). Whereas the *P* face elements of absorptive cell tight junctions were observed as strands with only occasional short focal interruptions (Fig. 4*A*), the *P* face elements of some villus goblet cell tight junctions consisted largely of widely spaced individual *IMPs* arranged in linear rows (Fig. 4*B*). Other villus goblet cell tight junctions were very deep with many strands but resembled a loosely woven stretched net in their appearance (Figs. 2*A* and 4*C*) in contrast to the highly organized chain-link fence appearance of absorptive cell tight junctions (Fig. 4*A*). Lastly, still other villus goblet cell tight junctions showed strands that paralleled the apical surface with very few vertically directed cross-linking strands (Fig. 4*D*).

Quantitation of tight junction depth and strand count confirmed the greater variability of junctional structure in villus goblet cells as compared to absorptive cells (Figs. 5 and 6). In 23% of villus goblet cell tight junctions, the strand count was less than 4 and in 30% the depth was less than 200 nm. In contrast, only 4% of absorptive cell tight junctions had strand counts less than 4 and only 9% had depth measurements less than 200 nm (Figs. 5 and 6). Villus goblet cell tight junctions had 17.2 free-ending abluminal strands per linear μm compared to only 1.4 for absorptive cell tight junctions.

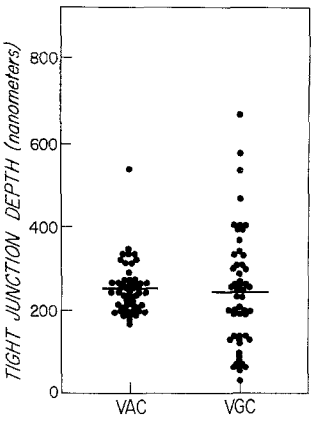

Fig. 5. The mean depth of tight junctions between villus absorptive cells (*VAC*) is similar to that of tight junctions associated with villus goblet cells (*VGC*) but tight junctions associated with villus goblet cells are much more variable in depth

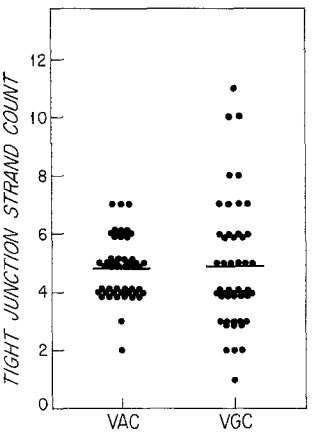

Fig. 6. The mean tight junction strand count is similar for villus absorptive cells (*VAC*) and villus goblet cells (*VGC*) but the range of strand counts for villus goblet cells is much greater than for villus absorptive cells

Passage of Tracers Into and Across Tight Junctions of Villus Epithelium

Lanthanum. Everted ileal sacs exposed to 1 mM $LaCl_3$ for 20 min showed focal dense lanthanum deposits along the microvillus border. In stained sections, the tight junctions of well-fixed absorptive cells did not show dense lanthanum deposits even when lanthanum was abundant along the brush border (Fig. 7*A*). In contrast, dense lanthanum deposits were found within tight junctions of approximately 5% of villus goblet cells. Independent of finding lanthanum in the junctional zone, the nonjunctional intercellular spaces surrounding 10–20% of goblet cells showed dense lanthanum deposits (Fig. 7*B*) while the intercellular spaces between adjacent undamaged absorptive cells did not. In unstained sections dense lanthanum deposits had the same distribution as in stained sections but, in addition, faint deposits could be recognized in the region of the tight junctions of occasional absorptive cells (Fig. 8) as well as in many villus goblet cell junctions. The dense lanthanum deposits associated with goblet cell tight junctions did not appear to be due to an increased affinity of goblet cell paracellular zones for lanthanum for similar dense deposits could also be seen occasionally in tight junctions between adjacent senescent absorptive cells at the extrusion zone on the tips of villi. There was no association between the degree of goblet cell mucin granule depletion and the presence or absence of lanthanum deposits in the tight junctions and paracellular spaces of villus goblet cells. Lanthanum deposits were apparent in pinocytotic vesicles and multivesicular bodies in some absorptive cells in unstained sections.

The brush borders of intestinal segments exposed *in vivo* for 60 min to 1 mM intraluminal $LaCl_3$ dis-

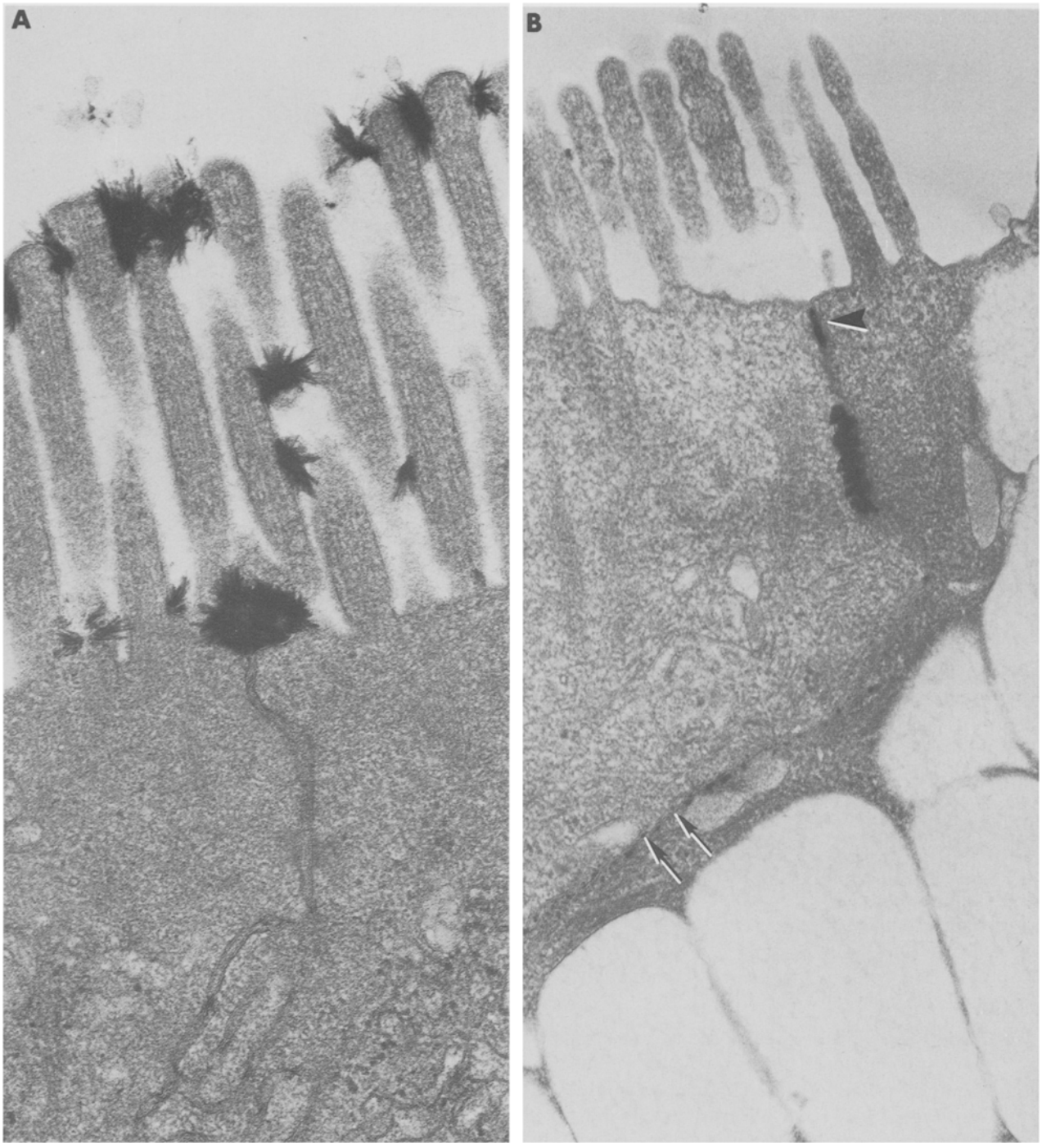

Fig. 7. (A) Electron micrograph of adjacent villus absorptive cells from ileal mucosa exposed to 1 mM $LaCl_3$ for 20 min prior to fixation. Although dense lanthanum precipitates are present in the brush border, none are apparent within the region of the tight junction or intercellular space. (61,500×) (B) Electron micrograph of a goblet cell from ileal mucosa exposed to 1 mM $LaCl_3$ for 20 min prior to fixation. Dense lanthanum deposits are present within the region of the tight junction (arrowhead) and intercellular space (arrows). (53,500×)

played fainter deposits of lanthanum than did everted sacs exposed to $LaCl_3$ *in vitro*. However, in stained sections dense lanthanum deposits could be appreciated in the paracellular space of approximately 5% of goblet cells. The paracellular spaces of villus absorptive cells did not contain dense lanthanum deposits but fainter deposits were once again appreciated in a few of these sites in unstained sections.

Everted ileal sacs which were prefixed for 45 min to 1 hr before their mucosal exposure to fixative con-

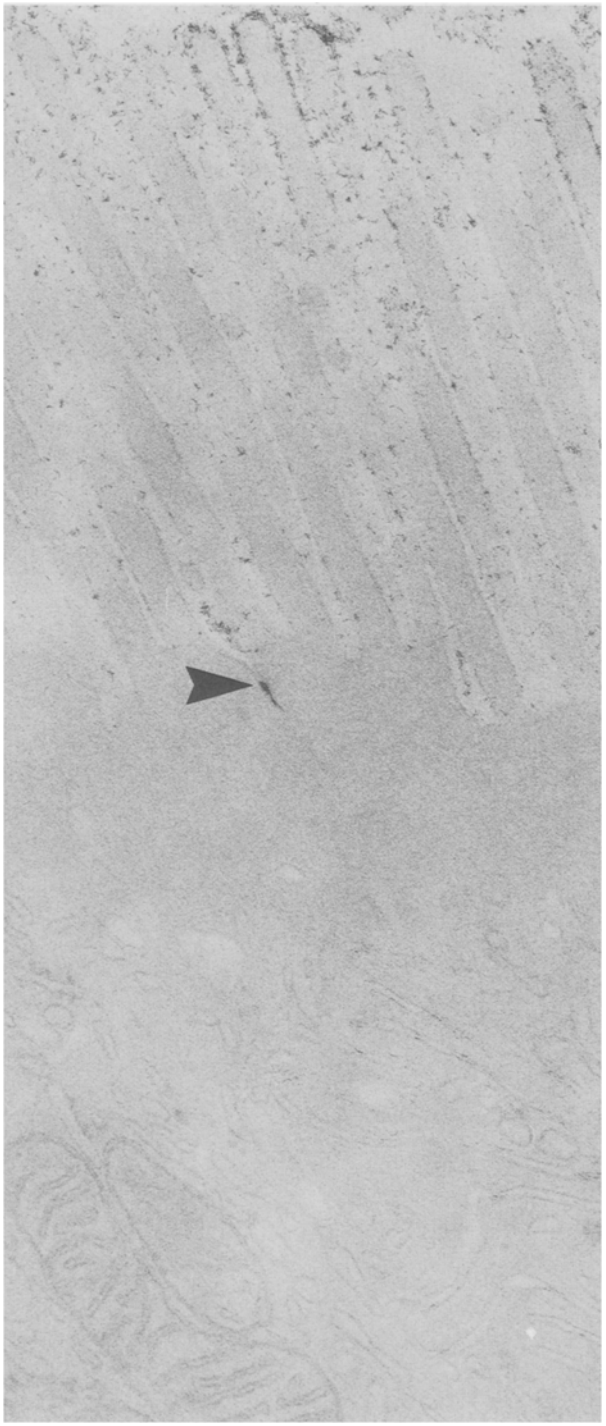

Fig. 8. Electron micrograph of unstained ileal mucosa exposed to $LaCl_3$ for 20 min prior to fixation. Faint lanthanum deposits can be appreciated in the superficial portion of the tight junction between two villus absorptive cells (arrowhead). (48,500×)

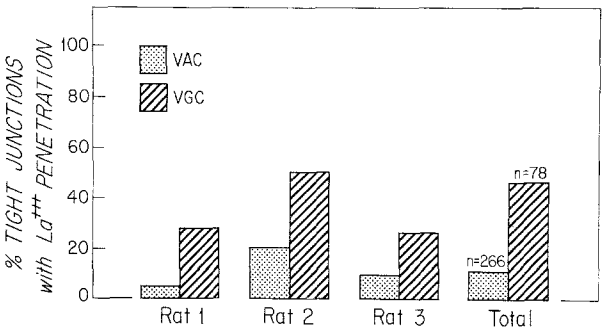

Fig. 9. Incidence of paracellular lanthanum precipitates found in unstained sections taken from prefixed mucosa exposed to 5 mM $LaCl_3$ for 1 hr. Paracellular lanthanum precipitates are more frequently found associated with villus goblet cells (*VGC*) than with villus absorptive cells (*VAC*)

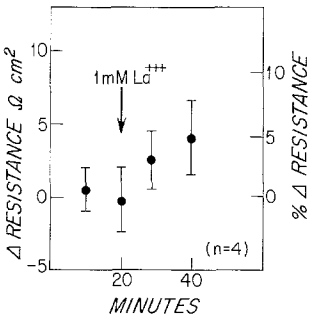

Fig. 10. Incremental change from paired control in transepithelial resistance after exposure of ileal mucosa to 1 mM $LaCl_3$. The vertical axis on the left indicates absolute change from paired control in $\Omega\,cm^2$ and the vertical axis on the right indicates percentage change from paired control. Lanthanum exposure does not result in a decrease in transepithelial resistance. Vertical bars indicate ± one standard deviation

taining 5 mM $LaCl_3$ for an additional 60 min showed dense aggregates of lanthanum interspersed with faint lanthanum precipitates along the microvillus border. Dense lanthanum deposits were again localized to the tight junction zone and paracellular space of some villus goblet cells. In unstained sections, fainter lanthanum deposits were recognized in only 14% of absorptive cell junctional zones whereas lanthanum deposits were evident in 42% of goblet cell junctional zones (Fig. 9). Lanthanum deposits were not visualized in apical vesicles or in multivesicular bodies of absorptive cells of pre-fixed intestine.

Examination of 10 freeze-fracture replicas prepared from tissues exposed to 1 mM La^{3+} *in vivo* for 20 min revealed absorptive and goblet cell tight junction structure comparable to that of unexposed tissue.

Exposure of ileal mucosa to 1 mM $LaCl_3$ in Ussing chambers for 20 min did not decrease transepithelial resistance. In fact, ileal sheets exposed to lanthanum showed a 5% increase in transepithelial resistance when compared to paired control ileal sheets which were not exposed to lanthanum (Fig. 10).

Prefixation for 1 hr did not decrease transepithelial resistance. Rather, transepithelial resistance of fixed tissues increased by approximately 20% during the 5-min period following addition of fixative to the serosal and mucosal baths and then gradually

decreased over the following 60 min to prefixation values (Fig. 11). Furthermore, the addition of 5 mM $LaCl_3$ the mucosal solution after 60 min of fixation did not produce a decrease in transepithelial resistance (Fig. 11).

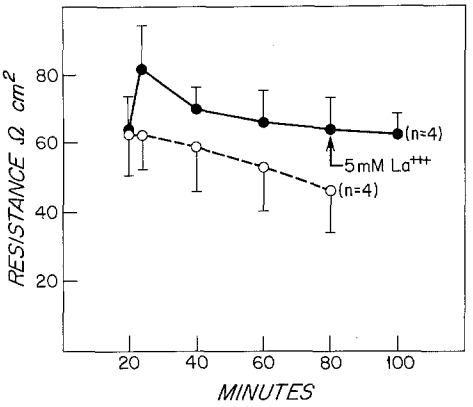

Fig. 11. Effect of fixation with 2% glutaraldehyde, 2.5% formaldehyde on transepithelial resistance of rat ileum. In comparison with unfixed paired control (broken line) fixation (solid line) does not lower transepithelial resistance. Furthermore, the addition of 5 mM mucosal $LaCl_3$ after fixation does not result in a significant alteration in transepithelial resistance. Vertical bars indicate ± one standard deviation

Barium. By light microscopy the ileal mucosa of sacs exposed first to $BaCl_2$ then to potassium rhodinozate showed diffuse pale red-brown staining of the mucosa. Heavy red-brown precipitates were localized to the apex of most villus goblet cells either as diffuse staining of the apical membrane or as a circle around the apex of the cell (Fig. 12*A*). In addition, lateral views of the epithelium revealed that occasional villus goblet cells had dense barium rhodinozate deposits in the area corresponding to the lateral intercellular space. (Fig. 12*B*). No such heavy deposits were seen in the region of intercellular spaces separating adjacent absorptive cells (Fig. 12).

Macromolecules. The microvillus borders of tissues exposed to either horseradish peroxidase or microperoxidase were heavily stained with reaction product. The density of reaction product was always greatest at the villus tips and decreased toward the base of the villus. The brush borders of ileal segments exposed to cytochrome *c* showed only small quantities of reaction product which were exclusively localized to the upper fourth of the villus. In tissues exposed to microperoxidase, reaction product was occasionally found in the paracellular space adjacent to damaged cells at the villus extrusion zones. However, even in areas

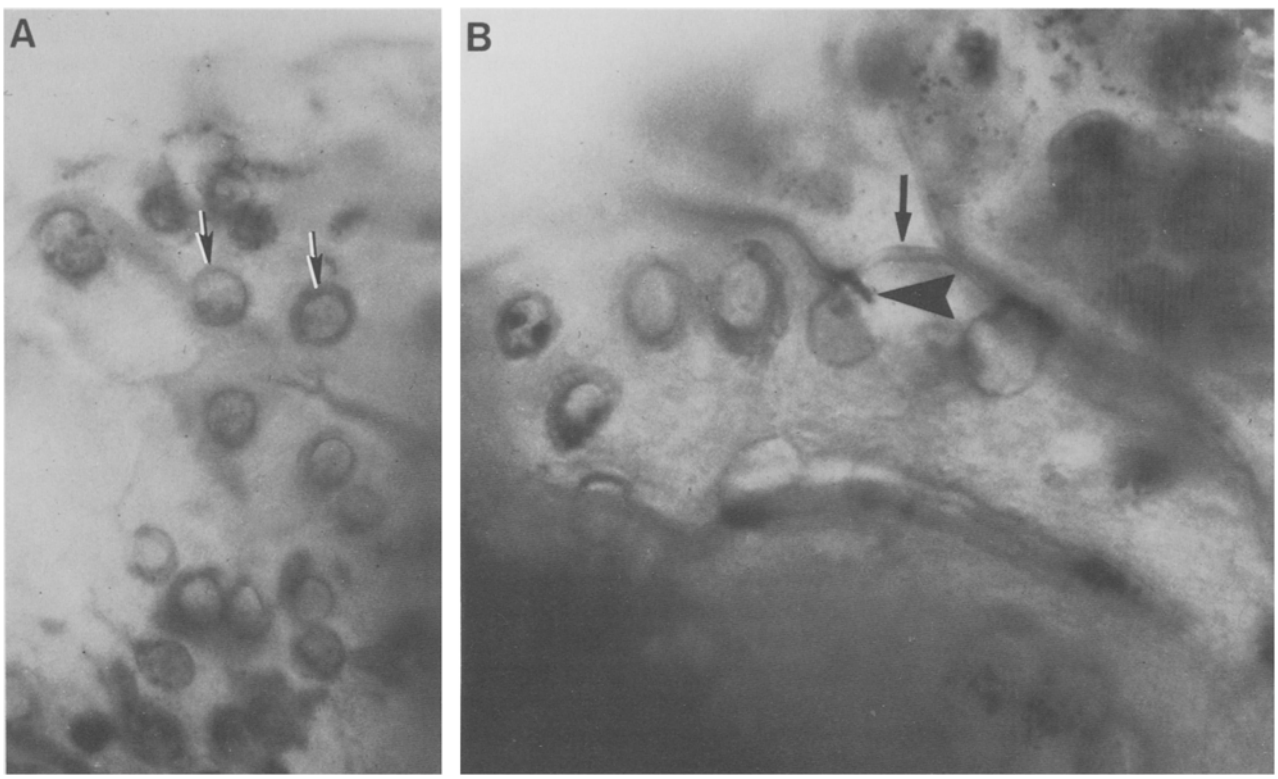

Fig. 12. Light micrographs of intact whole mounted villi sequentially exposed to 90 mM $BaCl_2$, fixative and saturated K rhodinozate. (*A*) Barium-rhodinozate deposits (red brown on the original slide) are present in the junctional zone of villus goblet cells (arrows). (550×). (*B*) Lateral view shows that barium-rhodinozate is found in the region of goblet cell paracellular spaces (arrowhead) but is not present between adjacent villus absorptive cells. The arrows indicate the microvillus border. (650×)

where the brush border was heavily stained, none of the macromolecular tracers utilized produced reaction product within the tight junction zones or the paracellular spaces surrounding undamaged absorptive cells or goblet cells.

Discussion

We show that the structural features of tight junctions associated with villus goblet cells in rat ileum are much more variable than those shared by adjacent absorptive cells. Some villus goblet cell tight junctions are shallow and consist of few strands. Others display additional structural features not usually seen in tight junctions between absorptive cells including extensive strand fragmentation, poor strand cross-linking and abundant aberrant abluminal strands. Furthermore, ionic lanthanum and barium penetrate a substantially greater percentage of villus goblet cell tight junctions than tight junctions between adjacent absorptive cells. Dense paracellular deposits of ionic tracers were almost exclusively associated with villus goblet cells. Although La^{3+} was sometimes endocytosed by unfixed cells, it is unlikely that it entered the paracellular spaces via the transcellular route. The percentage of paracellular spaces containing this tracer was comparable whether ileum was exposed to $LaCl_3$ prior to or after fixation.

In general, tight junction structure correlates with transepithelial resistance in a variety of other epithelia [4]. Tight junction structure and transepithelial resistance are also generally correlated with the ability of tight junctions to exclude lanthanum. For example, in the renal tubule, an increase in transepithelial resistance from proximal (5–7 $\Omega\,cm^2$, rat) [13] to distal tubule (350 $\Omega\,cm^2$, rat) [19] to collecting duct (867 $\Omega\,cm^2$, rabbit) [14] is paralleled by an increase in the number of tight junction strands from proximal (0–6, rat) to distal (2–11, rat) to collecting duct (6–14, rat) [29]. Furthermore, ionic lanthanum penetrates epithelial tight junctions of proximal and distal tubules but not those of collecting ducts [20, 34]. Toad urinary bladder has an extremely high (3,500 $\Omega\,cm^2$) transepithelial resistance [2] and its tight junctions are complex with 5–11 horizontal strands [4] that exclude ionic lanthanum from the paracellular space. However, when hyperosmotic stress is applied to the mucosal surface, transepithelial resistance drops, tight junctions develop structural abnormalities, and macromolecules penetrate into the tight junction [36, 37]. Similarly, hypertonic loads applied to frog skin produce a drop in transepithelial resistance which coincides with a large increase in transepithelial flux of ^{140}La [8]. The site of this increased permeability has been localized with colloidal lanthanum to the tight junctions which reside in the stratum granulosum [22]. Other epithelia with low resistance, like those of the proximal renal tubule are permeable to ionic tracers. After 1 hr of mucosal exposure to 1 mM ionic lanthanum, the majority of rabbit gallbladder (resistance – 30 $\Omega\,cm^2$) and about 50% of unfixed rabbit small intestinal (resistance – 42 to 61 $\Omega\,cm^2$) tight junctions were permeable to lanthanum [17]. That study, in which the unfixed ileal mucosa was exposed to 1 mM $LaCl_3$ for periods three times longer than our exposure period, did not comment on relative differences in lanthanum penetration dependent on epithelial cell type. Evidence for the relationship between junctional structure and permeability to small tracers also exists in nonmammalian vertebrates. In the gill of salt water adapted teleosts, chloride cells have tight junctions which consist of a single strand and are penetrated by colloidal lanthanum while tight junctions between respiratory cells have multiple strands and exclude colloidal lanthanum [31].

Although ionic lanthanum has been extensively used as a tracer to evaluate tight junction resistance to ionic flow, it is not physiologically inert. The glucose-stimulated transepithelial potential difference of rabbit small intestine gradually deteriorates during the 60 min following mucosal exposure to 1 mM $LaCl_3$ [17]. However, this effect is not related to nonspecific cytotoxicity or selective opening of the paracellular shunt for transepithelial resistance rises and remains above pre-exposure resistance for the entire period [17]. A small increase in resistance after mucosal exposure to 1 mM ionic lanthanum also occurs in rabbit gallbladder [17] and we demonstrate a similar alteration in rat small intestinal epithelium after 20-min exposure to 1 mM $LaCl_3$. We could not follow the transepithelial resistance for longer periods of time since the mucosal structure of rat small intestinal epithelium deteriorates more rapidly in Ussing chambers than does the epithelium of rabbit small intestine.

To examine the structure of rat mucosa after prolonged exposure to lanthanum we utilized everted sacs which were prefixed. This maneuver is apparently not associated with an increase in paracellular flow since transepithelial resistance, which in small intestine depends largely on paracellular ionic flow [11], actually increased. Similarly, Martinez-Palomo et al. [23] have recently demonstrated that prolonged aldehyde fixation does not decrease transepithelial resistance of monolayers of MDCK cells.

Since the ionic lanthanum marker might be displaced by diffusion during fixation, dehydration and embedment, we also utilized the barium rhodinozate technique which permits tissue examination within 35 min of barium exposure and within 1–2 min of rhodinozate labeling [6, 38]. Like ionic lanthanum,

ionic barium selectively penetrated the paracellular space surrounding goblet cells. We conclude that a) the highly variable and often disorganized structure of villus goblet cell-associated tight junctions as assessed by freeze-fracture, b) the preferential penetration of ionic lanthanum into paracellular spaces adjacent to a subpopulation of villus goblet cells, and c) the preferential localization of barium rhodinozate to the junctional zone and paracellular space of villus goblet cells strongly suggest that there is a subpopulation of villus goblet cells with tight junctions that serve as sites of relatively high ionic permeability.

Epithelia might be divided into two major groups (based on the cell types lining them): those epithelia composed of relatively homogenous cell populations, for example, proximal renal tubule and choroid plexus, and those with heterogeneous cell populations, for example, mammalian trachea, teleostean fish gill and mammalian small intestine. Unlike the homogenous epithelia where tight junction structure from cell to cell is quite uniform [24, 29], in structurally heterogeneous epithelia tight junction structure has been shown to vary dramatically from one cell type to another [18, 31, 32]. Since the relationship between the number of horizontal tight junction strands and transepithelial resistance may be logarithmic [3], cells with junctions consisting of only a few strands scattered throughout an otherwise tight epithelium might have a profound influence on overall transepithelial resistance. Thus, measurements of mean tight junction structure in heterogeneous epithelia might correlate less well with transepithelial resistance than similar measurements of junctional structure in epithelia with homogenous cell populations. This is emphasized by recent studies in cultured monolayers of MDCK cells in which the transepithelial resistance is relatively low (70–200 Ω cm^2) although the majority of tight junctions consist of 8–10 horizontal strands [1]. However, intermixed within this major population of well-developed tight junctions is a subpopulation of tight junctions with only 1–2 strands. When the surface of the monolayer is scanned with microelectrodes, long junctional segments of high resistance are focally interrupted with sites of low resistance [1], which presumably correspond to those tight junctions with few strands.

Based on the data we present, it is possible that resistance across villus epithelium might be inordinately affected by a subpopulation of low resistance sites around villus goblet cells. In 1-μm sections of rat ileum, we find that goblet cells constitute 12% (49 out of 400) of villus epithelial cells, thus the percentage of villus junctional area related to goblet cells is approximately 10%. However, it is not clear what percentage of these sites might be highly conductive compared to absorptive cell tight junctions: we find 10–15% of goblet cell tight junctions permeable to La^{3+} by ultrastructural techniques, but find most goblet cell tight junctions permeable to Ba^{2+} using light microscopy. Thus, the frequency with which enhanced permeability of goblet cell tight junctions is documented depends on the tracer and the technique used for its demonstration.

Variability in tight junction structure might explain, at least in part, why a heterogeneous epithelium like the small intestine might seem extraordinarily leaky given its mean junctional structure [21]. We have shown previously that tight junctions between undifferentiated crypt cells are less uniform and on the average are less deep and have fewer strands than do those between villus absorptive cells [18]. In the present report we document that tight junctions associated with goblet cells also have structural and probably functional variability which contrasts to those of absorptive cells. Thus, measurement of transepithelial resistance in the small intestine in all likelihood reflects the sum of subpopulations of tight junctions and paracellular pathways which vary in resistance.

This work was supported by research grants AM 27927 and AM 17537 from the National Institutes of Health. Dr. Madara was supported in part by National Research Service Institutional Training Program AM 07121 and National Research Service Award AM 06192. We are grateful fo Dr. Marian Neutra for critically reviewing the manuscript.

References

1. Cereijido, M., Stefani, E., Martinez-Palomo, A. 1980. Occluding junctions in a cultured transporting epithelium: Structural and functional heterogeneity. *J. Membrane Biol.* **53**:19–32
2. Civan, M.M., Frazier, H.S. 1968. The site of the stimulatory action of vasopressin on sodium transport in toad bladder. *J. Gen. Physiol.* **51**:589–605
3. Claude, P. 1978. Morphological factors influencing transepithelial permeability: A model for the resistance of the zonula occludentes. *J. Membrane Biol* **39**:219–232
4. Claude, P., Goodenough, D.S. 1973. Fracture faces of zonulae occludentes from "tight" and "leaky" epithelia. *J. Cell Biol.* **58**:390–400
5. Cornell, J.S., Meister, A. 1976. Glutathione and gamma-glutamyl cycle enzymes in crypt and villus tip of cells of rat jejunal mucosa. *Proc. Natl. Acad. Sci. USA* **73**:420–422
6. Cotran, R.S., Nicca, C. 1968. The intercellular localization of cations in mesothelium. A light and electron microscopic study. *Lab. Invest.* **18**:407–415
7. Dawson, I., Pryse-Davies, J. 1963. The distribution of certain enzyme systems in the normal human gastrointestinal tract. *Gastroenterology* **44**:745–760
8. Erlij, D., Martinez-Palomo, A. 1972. The opening of tight junctions in frog skin by hypertonic urea solutions. *J. Membrane Biol.* **9**:229–240
9. Feder, N. 1970. A heme-peptide as an ultrastructural tracer. *J. Histochem. Cytochem.* **18**:911–913
10. Field, M. 1981. Secretion by the small intestine. *In*: Physiology of the Gastrointestinal Tract. L. Johnson, J. Christensen, M.I.

Grossman, E.D. Jacobson, and S.G. Schultz, editors. pp. 963–982. Raven Press, New York
11. Frizzell, R.A., Schultz, S.G. 1972. Ionic conductances of extracellular shunt pathway in rabbit ileum. Influence of shunt on transmural sodium transport and electrical potential differences. *J. Gen. Physiol.* **59**:318–346
12. Graham, R.C., Karnovsky, M.J. 1966. The early stages of absorption of injected horseradish peroxidase in the proximal tubules of mouse kidney: Ultrastructural chemistry by a new technique. *J. Histochem. Cytochem.* **14**:291–300
13. Hegel, U., Fromter, E., Wisk, T. 1967. Der elektrische Wandwiderstand des proximalen Konvolutes der Rattenniere. *Pfluegers Arch. Gesamte Physiol.* **292**:274–290
14. Helman, S.I., Grantham, J.J., Burg, M.B. 1971. Effect of vasopressin on electrical resistance of renal cortical collecting tubules. *Am. J. Physiol.* **220**:1825–1832
15. Karnovsky, M.J. 1965. A formaldehyde-glutaraldehyde fixative of high osmolality for use in electron microscopy. *J. Cell Biol.* **27**:137a. (Abstr.)
16. Karnovsky, M.J., Rice, D.F. 1969. Exogenous cytochrome *c* as an ultrastructural tracer. *J. Histochem. Cytochem* **17**:751–753
17. Machen, T.E., Erlij, D., Wooding, F.B.P. 1972. Permeable junctional complexes. The movement of lanthanum across rabbit gallbladder and intestine. *J. Cell Biol.* **54**:302–312
18. Madara, J.L., Trier, J.S., Neutra, M.R. 1980. Structural changes in the plasma membrane accompanying differentiation of epithelial cells in human and monkey small intestine. *Gastroenterology* **78**:963–975
19. Malnic, G., Giebisch, G. 1972. Some electrical properties of distal tubular epithelium in the rat. *Am. J. Physiol.* **223**:797–808
20. Martinez-Palomo, A., Erlij, D. 1973. The distribution of lanthanum in tight junctions of the kidney tubule. *Pfluegers Arch* **343**:267–272
21. Martinez-Palomo, A., Erlij, D. 1975. Structure of tight junctions in epithelia with different permeability. *Proc. Natl. Acad. Sci. USA* **72**:4487–4491
22. Martinez-Palomo, A., Erlij, D., Bracho, H. 1971. Localization of permeability barriers in the frog skin epithelium. *J. Cell Biol.* **50**:277–287
23. Martinez-Palomo, A., Mexa, I., Beaty, G., Cereijido, M. 1980. Experimental modulation of occluding junctions in a cultured transporting epithelium. *J. Cell Biol.* **87**:736–745
24. Møllgård, K., Malinoska, D.H., Saunders, N.R. 1977. Lack of correlation between tight junction morphology and permeability properties in developing choroid plexus. *Nature (London)* **264**:293–295
25. Munck, B.G. 1972. Effects of sugar and amino acid transport on trans-epithelial fluxes of sodium and chloride of short circuited rat jejunum. *J. Physiol. (London)* **223**:699–717
26. Nabeyama, A., LeBlond, C.P. 1974 "Caveolated cells" characterized by deep surface invaginations and abundant filaments in mouse gastrointestinal epithelium. *Am. J. Anat.* **140**:147–166
27. Nordstrom, C., Dahlqvist, A. 1972. Quantitative distribution of some enzymes along villi and crypts of human small intestine. *Scand. J. Gastroenterol.* **8**:407–416
28. Padykula, H.A., Strauss, E.W., Ladman, A.J., Gardner, F.H. 1961. A morphologic and histochemical analysis of the human jejunal epithelium in nontropical sprue. *Gastroenterology* **40**:735–765
29. Pricam, C., Humbert, F., Perrelet, A., Orci, L. 1974. A freeze-etch study of the tight junctions of the rat kidney tubules. *Lab. Invest.* **30**:286–291
30. Roggin, G.M., Banwell, J.G., Yardley, J.H., Hendrix, T.R. 1972. Unimpaired response of rabbit jejunum to cholera toxin after selective damage to villus epithelium. *Gastroenterology* **63**:981–989
31. Sardet, C., Pisam, M., Maetz, J. 1979. The surface epithelium of teleostean fish gills cellular and junctional adaptations of the chloride cell in relation to salt adaptation. *J. Cell Biol.* **80**:96–117
32. Schneeberger, E.F. 1980. Heterogeneity of tight junction morphology in extrapulmonary and intrapulmonary airways of the rat. *Anat. Rec.* **198**:193–208
33. Tice, L.W., Carter, R.L., Cahill, M.B. 1979. Changes in tight junctions of rat intestinal crypt cells associated with changes in their mitotic activity. *Tissue Cell* **11**:293–316
34. Tisher, C.C., Yarger, W.E. 1973. Lanthanum permeability of the tight junction (zonula occludens) in the renal tubule of the rat. *Kidney Int.* **3**:238–250
35. Trier, J.S., Madara, J.L. 1981. The functional morphology of the mucosa of the small intestine. *In*: Physiology of the Gastrointestinal Tract. L. Johnson, J. Christensen, M.I. Grossman, E.D. Jacobson, and S.G. Schultz, editors. pp. 925–961. Raven Press, New York
36. Wade, J.B., Karnovsky, M.J. 1974. Fracture faces of osmotically disrupted zonulae occludentes. *J. Cell Biol.* **62**:344–350
37. Wade, J.B., Revel, J.P., DiScala, V.A. 1973. Effect of osmotic gradients on intercellular junctions of the toad bladder. *Am. J. Physiol.* **224**:407–415
38. Waterhouse, D.F. 1950. The occurrence of barium and strontium in insects. *Austral. J. Sci. Res. Ser. B.* **5**:144–162

Received 17 August 1981; revised 27 October 1981